ELSEVIER

Diamond and Related Materials 10 (2001) 915–919

DIAMOND AND RELATED MATERIALS

www.elsevier.com/locate/diamond

DLC films prepared by electron evaporation of graphite in an ECR plasma

S. Muhl[a,*], E. Camps[b], L. Escobar-Alarcón[b], O. Olea[c], M. Miki[d], N.A. Morrison[e]

[a] *Instituto de Investigaciones en Materiales, U.N.A.M., México, D.F., Mexico*
[b] *Instituto Nacional de Investigaciones Nucleares, Edo. de México, Mexico*
[c] *U.A.E.M, Edo. de México, Mexico*
[d] *C.I.M.A.V., Chihuahua, Coahila, Mexico*
[e] *Department of Engineering, University of Cambridge, Cambridge, England, UK*

Abstract

Films of diamond-like carbon (DLC) have been prepared by a novel electron evaporation scheme in an argon plasma within a linear microwave ECR reactor. The electrons present in the high density ECR plasma are attracted to a biased graphite rod to such an extent that the carbon is thermally evaporated. The argon ions bombard the substrate with an energy determined by the plasma potential and the substrate bias. However, the plasma potential is determined by the size of the graphite rod as well as the applied voltage. The films have been analysed using the following techniques: profilometry (thickness and residual stress); ellipsometry (refractive index and thickness); Raman spectroscopy (atomic bonding); UV-Vis spectrophotometry (bandgap), PEELS (C sp^3), EDX and RBS (chemical analysis). The results are discussed in terms of the knock-on subplantation model [Rad. Effects Defects Solids, 142 (1997) 63] and the recently published interpretation of the Raman spectra of carbon films [Phys. Rev. B, 61 (2000) 14095].

Keywords: Diamond-like carbon; ECR plasma; Ellipsometry

1. Introduction

Plasma assisted deposition processes are used extensively to study the preparation of both new materials, as well as, more commonplace compounds with improved properties. The preparation of thin films of diamond-like carbon [2] is a notable example of a material which is extremely difficult to synthesis without the use of plasmas. When plasma assisted chemical vapour processes are used, the resulting deposits normally contain significant quantities of hydrogen, and the term DLC is often used to describe this hydrogenated form of diamond-like carbon [3,4]. The non-hydrogenated form of carbon, as prepared from solid carbon sources, is referred to as tetrahedrally bonded amorphous carbon (ta-C). In both cases, DLC and ta-C, the material properties are determined by the relative amounts of sp^1, sp^2 and sp^3 bonding between the carbon atoms [5].

It is generally accepted that the transformation of part of the sp^2 bonded carbon, which is the configuration which initially forms on the surface of the deposit, to the sp^3 form occurs by the densification and/or introduction of above average levels of localised energy in the subsurface region of the coating. This process is caused by the incidence of medium energy, 50–250 eV,

* Corresponding author. Tel.: +52-5622-4736; fax: +52-5616-1251.
E-mail address: muhl@servidor.unam.mx (S. Muhl).

0925-9635/01/$ - see front matter
PII: S0925-9635(00)00557-4

carbon species, as long as low substrate temperatures are used to reduce the thermal relaxation of the densification process [6].

The main techniques that have been used to make DLC films include: mass selected ion beam deposition (MSIBD) [7–10], plasma CVD [11–13], magnetron sputtering [14–16], filtered vacuum cathode arc deposition (FVCA) [17–19] and pulsed laser deposition [20–22], with substrate biasing to control the energy of the incident carbon ions. MSIBD is a highly sophisticated technique but is not readily useable as an industrial method and PECVD can only be used to prepare a-C:H. The disadvantage of magnetron sputtering is that the plasma density is normally quite low, $\sim 10^8$–10^9 cm^{-3}, and therefore it is difficult to get sufficient bombardment of the growing film. Both the arc and laser methods suffer from problems related to the inclusion of macro particles, emitted from the carbon target, into the deposit. However, both techniques have the advantage that only carbon species and electrons are incident on the substrate. In this paper we describe the use of a novel plasma assisted deposition method involving a solid source of carbon which results in films of reduced macroparticle content when compared with laser ablation and filtered arc techniques.

2. Experiment

A high density, low pressure argon plasma ($n_e \sim 10^{10}$–10^{11} cm^{-3} and 4×10^{-4} Torr) was generated in our microwave ECR system, the details of which have been published elsewhere [23]. Basically, the ECR condition is established in one section of the apparatus and a high-density plasma beam, approximately 6 cm in diameter, is directed into the deposition chamber by a magnetic field gradient generated by three electromagnetic coils. Electrons are extracted from this plasma to thermally evaporate carbon from a positively biased graphite rod. The water-cooled and biased graphite rod was placed horizontally and perpendicular to this plasma beam, as shown in the Fig. 1. The optimum lateral position of the rod depends on the plasma conditions as well as the electron current and ion energy required for a given experiment. Indeed, the rod position and length are additional experimental control parameters. The substrates were placed in front of, and in line with, the axis of the graphite rod, again as shown in Fig. 1. The substrate holder is water-cooled and electrically isolated from the system wall (the maximum observed substrate temperature was 80°C). Experiments were performed with the substrates grounded, floating and using both positive and negative biasing conditions (V_{subs}), -80 to $+25$ V. The substrate holder was approximately 3 cm from the edge of the plasma.

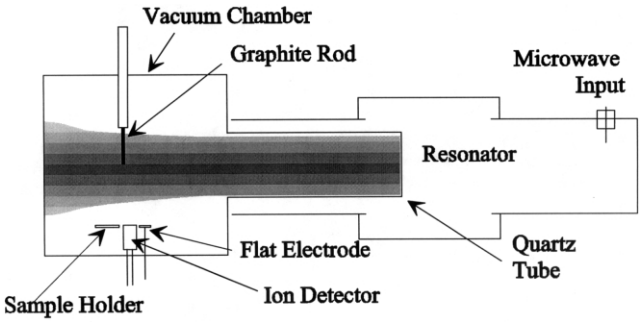

Fig. 1. Schematic of the ECR microwave plasma assisted deposition system showing the orientation of the carbon source and the substrate with respect to the plasma.

Experiments were performed in an argon plasma at 4×10^{-4} torr and microwave powers of between 320 and 450 W, for various rod positions and lengths, with bias voltages (V_{graf}) of the graphite rod, 100–400 V, and adjustment of the magnetic fields to control the current in the graphite rod, I_{graf}.

The plasma characteristics were measured using an electrostatic probe and the ion energy, I_E, and flux, I_F, were determined using a Faraday cup analyser with an electron expelling electrode and a variable ion retarding potential.

Additionally, the plasma emission spectra was measured using a Minuteman 305SLP monochromator equipped with a fast intensified charge coupled device (Princeton Instruments ICCD-MAX 1024E), working in its shuttered mode. The monochromator has a 0.5-m focal length, a 1200-g/mm grating with a 14-μm slit. The light emitted by the plasma was collected by a UV-Vis fibre bundle through a quartz window in the reactor. In this configuration a spectral window of 40 nm with a 3-Å resolution was observed.

The films were prepared on cleaned 1×1 cm pieces of (100) silicon and Corning 7059 borosilicate glass. The deposits were characterised by ellipsometry (Gaertner Model L, 117) to obtain the thickness and refractive index. The bandgap was calculated from the absorption spectra obtained using a UV-Vis spectrophotometer (Shimadzu Model UV-260) and a profilometer (Sloan Dektak IIA) was used to the thickness and residual stress through the application of the beam bending technique. The Raman spectra were recorded with a Spex 1403 double monochromator using the 514.5 nm line of an argon laser in a backscattering configuration. The signal was detected with a photomultiplier and a standard photon counting system. A Leica-Cambridge Stereoscan 440 scanning electron microscope equipped with an energy dispersive X-ray analyser (EDX) were used for the elemental composition measurements and to determine the film topography. The RBS measurements were performed using a tandem Van de Graaf accelerator to generate a 2-MeV

deuterium beam which was retrodispersed at an angle of 150°. Finally, the EELS analysis was carried out using a DIGI-PEELS 766 spectrometer mounted on a CM200 TEM.

3. Results and discussion

3.1. The evaporation and deposition processes

The carbon was thermally evaporated from the graphite rod by the electrons extracted from the plasma. The temperature of the rod was controlled by the product of the electron flux and the electron energy. The energy is therefore determined by the width and potential across the sheath surrounding the rod. The sheath width was mainly dependent on the plasma density and electron temperature and increased only slightly for $V_{graf} > 100$ V since this condition corresponds to a Langmuir probe biased to positive voltages greater than the plasma potential, i.e. electron saturation. Therefore, for a given electron (plasma) density, the rod temperature is controlled by the sheath potential as this controls the electron energy. The variation of the plasma potential, V_{pl}, with V_{graf} depended upon the size, and to some extent the position of, the graphite rod. If a rod larger than 2 cm was used, the plasma was strongly perturbed and V_{pl} increased sublinearly with V_{graf}. However, for rods less than this size V_{pl} increased to ~ 60 V as V_{graf} was increased to ~ 100 V and then remained approximately constant.

Initially, we considered that the high electron flux incident on the graphite ($\sim 2 \times 10^{20}$ electrons/cm^2/s) would be sufficient to ionise a significant fraction of the emitted carbon atoms. However, the OES, ion detector measurements and the measured characteristics of the deposits indicated that the carbon species present in the plasma and those incident on the substrate are neutral atoms having energies typical of thermally emitted atoms. The carbon film precursors are accompanied by a considerable flux of argon ions. With $V_{graf} = 0$, the Ar^+ energy incident on the substrate is 8–10 eV depending on the plasma conditions. For a large graphite rod the energy is dependent on V_{graf} and can be as large as 250 eV; for smaller rods E_{Ar^+} increases to ~ 60 eV as V_{graf} is increased to 100 V and is approximately constant thereafter. It should also be noted that carbon evaporation was not observed until V_{graf} exceeded a minimum of 250 V.

From the measured deposition rate and the plasma density we estimated that the if C^+ ions were present in the plasma then the ion current seen by the ion detector would be approximately 10% of the Ar^+ ion current. Moreover, because of the difference in ion mass and ion acceleration processes for the Ar^+ and C^+ species (the Ar^+ energy is determined by $V_{pl} - V_{subs}$, whereas the C^+ energy would be more dependent on $V_{graf} - V_{pl}$) two groups of ion signals would be observable in the ion detector spectra. Similarly, the only detectable carbon related OES signal was the 516.5 nm line corresponding to the neutral C_2 dimer. Thus, the film growth process can be described by the deposition of low energy C neutrals accompanied by higher energy Ar^+ ion bombardment.

The compositional analysis results obtained from RBS, EDX and PEELS indicated that the films contained only carbon with trace amounts, $< 1\%$, of argon when high Ar^+ energies were used. In addition, SEM micrographs taken during the EDX analysis demonstrated a low macroparticle density at the surface of our films (approx. 3.3×10^{-3} μm^2). However, sputtering of the substrate was observed if the Ar^+ energy was above an approximate threshold of 80 eV. Therefore, in relation to the discussion of the plasma perturbation presented above, sputtering was found if a long graphite rod was used with high V_{graf} voltages and if the substrate was negatively biased for almost all rod sizes and plasma configurations. Under conditions where minimal sputtering was observed the final film thickness was found to corresponded well with the amount of carbon evaporated when the geometric effects and the density differences between the graphite and the deposit were taken into account. Furthermore, the deposition rate was dependant on the magnitude of the power dissipated in the graphite rod (ca. 0.056–0.31 nm/s for applied graphite powers of 150–185 W).

3.2. Film characterisation

The Raman spectra exhibited the commonly observed D and G peaks associated with zone centre phonons of E_{g2} symmetry and the K-point phonons of A_{1g} symmetry, respectively. The relation between the G peak position and the ratio of the Gaussian fitted areas of the D and G peaks is presented in Fig. 2. As can be seen the G peak position moves from ~ 1540 to ~ 1580 cm^{-1} as the $I(D)/I(G)$ ratio increases from ~ 1.9 to ~ 3.4. Referring to the work of Ferrari and Robertson our Raman data indicate that these films should have an sp^3 carbon content in the range of 5–15%. This result is also supported by the PEELS measurements which show an sp^3 carbon content of between 10 and 20% and a density, calculated from the plasmon energy of between 1.48 and 1.61 g/cm^3; values of which are typical for low-density, highly sp^2 bonded amorphous carbon films. Similarly, the optical bandgap (Tauc) of the majority of the films were found to be between 0.4 and 1.2 eV and the residual stress values were all found to be less than 1 GPa.

3.3. Modified knock-on subplantation model

The film deposition process was also described using

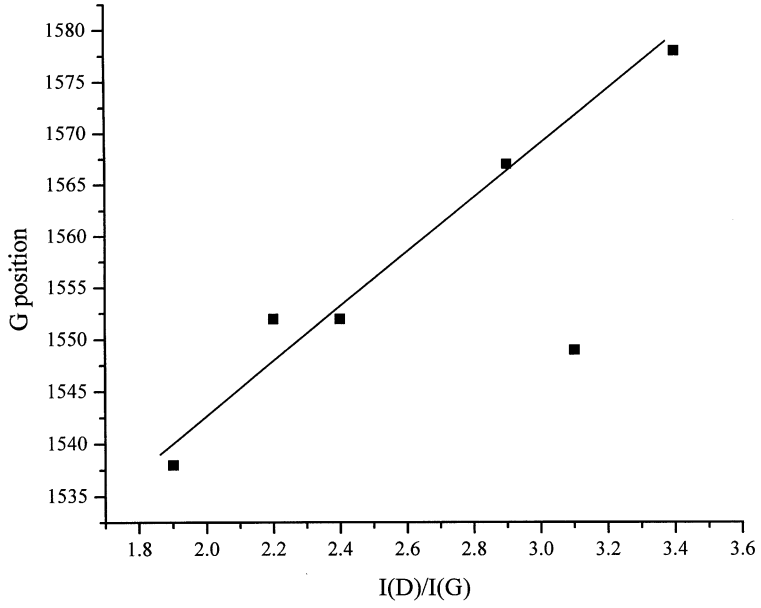

Fig. 2. A plot of the Raman G peak position vs. the $I(D)/I(G)$ ratio.

a modified knock-on subplantation mechanism. As a foundation the mechanism proposed by Robertson [1] was adapted to include affects associated with the relaxation of the subplanted layer through the recombination of the forward sputtered atoms and defects generated during the knock-on process. This model can be described by,

$$n = \frac{f}{1 + \alpha + \beta}$$

where n is related to the density increment of the subplanted layer, f is the flux of carbon atoms forward sputtered from the surface, α is the recombination relaxation constant experimentally fitted to a value of 5.4×10^{-3} and β is the thermal spike-induced relaxation factor. In addition,

$$f = aE_{\text{ion}}^{1/2} \qquad \beta = 0.016p\left(\frac{E_{\text{ion}}}{E_{\text{o}}}\right)^{5/3}$$

where a is a constant derived from the argon ion sputter yield of carbon, E_{ion} is the argon ion energy, p is a material constant of order 0.1 and E_{o} is the diffusion activation parameter (3.1 eV). As in the original Robertson model, these equations can be used to describe the incremental change in deposited film mass density as follows:

$$\frac{\Delta\rho}{\rho_{\text{o}}} = \frac{f\phi'}{1 - f\phi' + \alpha + \beta}$$

where $\Delta\rho$ is the change in mass density, ρ_{o} is the uncompressed mass density (1.2 g/cm^3), ϕ' is the argon ion to neutral carbon flux ratio and f, α and β have the same meanings as described above. This equation was used to generate a plot of the predicted mass density as a function of ion energy and is shown in Fig. 3 along with the experimental mass densities obtained from the PEELS measurements. Close agreement between the theoretical and experimental data was obtained using an ion to neutral flux ratio of 7.5:1 which is in reasonable agreement with the coarse estimation of this ratio (10:1) from the ion detector measurements and the deposition rates referred to above. The subtle difference in predicted mass density for the sample prepared using an ion energy of 15 eV can be attributed to a somewhat higher ion to neutral flux ratio due to the use of an increased plasma density. As a secondary result of this analysis it was possible to predict, from the ion flux, the plasma density with this yielding values of between 3×10^{10} and 2×10^{11} cm^{-3}. This is again in good accordance with results obtained from Langmuir probe analysis of microwave ECR argon plasmas in this experimental setup and reported elsewhere [24].

Within the present experimental setup, the plasma density is insufficient to result in an ion to neutral flux ratio greater than $\sim$10:1. This therefore places significant limits on the maximum degree of densification of the deposited material obtained. However, the use of a newly constructed ECR deposition system and the use of plasma densities greater than 2×10^{11} cm^{-3}, a V_{graf} value of $\sim$250 V (the threshold required for electron assisted carbon evaporation from the graphite rod) and ion energies below the sputtering threshold at $\sim$80 eV should permit the deposition of films of densities in excess of 1.6 g/cm^3.

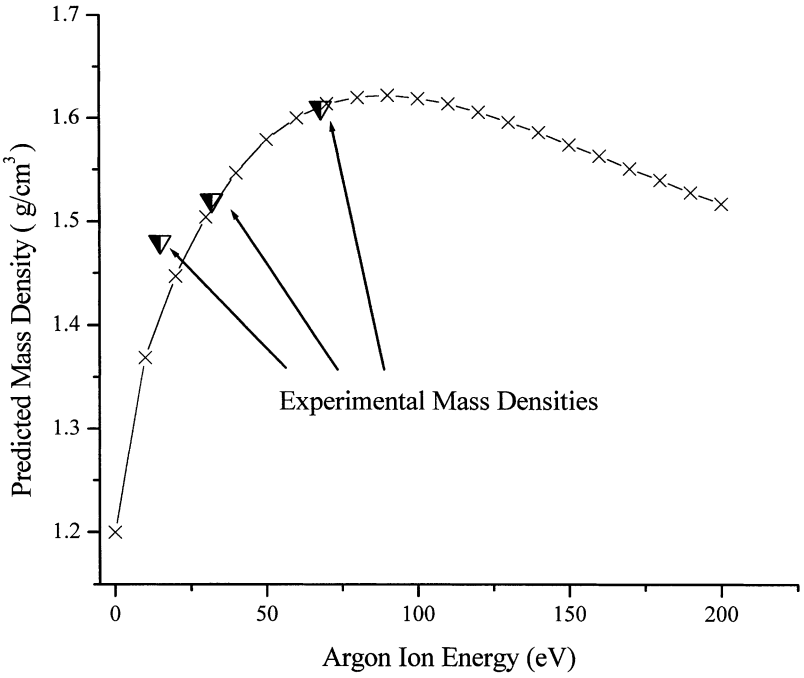

Fig. 3. A plot of both the predicted and experimental mass densities as a function of Argon ion energy.

4. Conclusions

We have demonstrated that the ECR plasma-assisted evaporation of graphite can be used to deposit amorphous carbon films with an sp^3 content and mass density of $\sim 20\%$ and 1.61 g/cm^3, respectively. The deposition process was accurately described using a modified knock-on subplantation model which permitted calculation of the observed mass densities to within $\pm 2\%$ of the experimental values. Furthermore, the model has provided significant insight as to why the present experimental setup has resulted in the formation of highly sp^2 bonded amorphous carbon films. It has also helped elucidate a method by which the sp^3 content and mass density of the films may be further improved.

Acknowledgements

The authors wish to acknowledge the financial support of the following projects CONACyT No. 27676E and DGAPA No. IN 114998.

References

[1] J. Robertson, Rad. Effects Defects Solids 142 (1997) 63–90.
[2] S.R.P. Silva, J. Robertson, W.I. Milne and G.A.J. Amaratunga, (eds.) Amorphous carbon: state of the art, Proc. 1st Int. SMAC'97, World Scientific, Singapore (1998).
[3] M. Weiler et al., Phys. Rev. B. 53 (1996) 1594–1608.
[4] S. Sattel, J. Robertson, H. Ehrhardt, J. Appl. Phys. 82 (1997) 4566–4576.
[5] Dresselhaus, A.S., Kalish, R. Ion Implantation in Diamond, Graphite and Related Materials, H.K.V. Lotsch (ed.) Springer series in Materials Science, 22 (1992) 3–25.
[6] Y. Lifshitz, G.D. Lempert, E. Grossman, Phys. Rev. Lett. 72 (1994) 2753–2756.
[7] W. Moller, Appl. Phys. Lett. 59 (1991) 2391–2393.
[8] Y. Lifshitz et al., Diamond Relat. Mater. 3 (1994) 542–546.
[9] E. Grossman et al., Appl. Phys. Lett. 68 (1996) 1214–1216.
[10] J. Kulik et al., J Appl. Phys. 76 (1994) 5063–5069.
[11] G.J. Vandentop et al., J Vac. Sci. Technol. A 9 (1991) 2273–2278.
[12] A. Raveh, J.E. Klemberg-Sapieha, L. Martinu, M.R. Wertheimer, J Vac. Sci. Technol. A 10 (1992) 1723–1727.
[13] G.J. Vandentop et al., Phys. Rev. B 41 (1990) 3200–3210.
[14] H. Murzin et al., Mat. Res. Soc. Symp. Proc. 498 (1998) 153–158.
[15] N. Sauvides, J Appl. Pkvs. 58 (1985) 518–521.
[16] J. Schwan et al., J. Appl. Phys. 79 (1996) 1416–1422.
[17] R. Lossy et al., J. Appl. Phys. 77 (1995) 4750–4756.
[18] P.J. Fallon et al., Phys. Rev. B 48 (1993) 4777–4882.
[19] M. Chhowalla et al., J Appl. Phys. 81 (1997) 139–145.
[20] A.A. Voevodin, M.S. Donley, Surf. Coat. Technol. 82 (1996) 199–213.
[21] J.J. Cuomo et al., J Vac. Sci. Technol. A 10 (1992) 3414–3418.
[22] D. Pappas et al., J Appl. Phys. 71 (1992) 5675–5684.
[23] S. Muhl, E. Camps, L. Escobar-Alcaron and O. Olea, to be published in Thin Solid Films, 2000.
[24] E. Camps, S. Muhl, O. Alverez-Fregoso, J.A. Juarez-Islas, O. Olea, S. Romero, J. Vac. Sci. Technol. A 17 (1999) 2007–2014.